CONCERNING THE MECHANISM AND SELECTIVITY OF PALLADIUM(II)-CATALYZED AEROBIC OXIDATION REACTIONS

Thesis by

Raissa M. Trend

In Partial Fulfillment of the Requirements for the Degree of

Doctor of Philosophy

California Institute of Technology

Pasadena, California

2006

(Defended 28 February, 2006)

ACKNOWLEDGEMENTS

"Sure...why not join a fledging synthetic organic group and work for a professor with slightly elevated expectations?" I said to myself four and a half years ago. As it turns out, it was a lucky choice for me; there was probably no better advisor I could have worked for than Brian Stoltz. I thank Brian for his attention and concern, his dedication to his group, and his high standards of excellence. It has been an invaluable experience for me to participate in the intellectual and scientific development of a young lab, and a privilege to have an advisor so willing to listen to (or at least tolerate) my opinions. He is always able to ask thoughtful questions, and to somehow keep track of so many projects. Brian's readiness to explore areas outside of his primary area of expertise played a major role in the outcome of my graduate career, and I am grateful to have had this freedom. He has been both a great mentor and a friend, a perhaps unusual combination to find in a graduate advisor. I am looking forward to seeing in what directions his interests and those of his students take the lab. Although I probably couldn't have realized what I was getting myself into when I joined the Stoltz lab, it has been an experience I will continue to learn from and appreciate for years to come.

I must also thank the other members of my committee for their amazing support and dedicated proposal reading and letter writing. Professor Bob Grubbs has continuously had insightful comments about my work, and he and his group contribute enormously to the special atmosphere of the Caltech chemistry department, whether through Nobel prizes or pub crawls. Professor John Bercaw's questions have always been helpful to this quasi-organometallic chemist, and my work wouldn't be where it is without the Bercaw group. While Professor Dennis Dougherty is the most recent addition to my committee, he has had a key role in determining the course of my future postdoctoral work, and it was a pleasure to sit in on his physical organic chemistry class.

I would also not be where I am today without my experience at UW-Madison in the labs of Professor Chuck Casey. His focus on the mechanisms of organometallic reactions has influenced me throughout my graduate career, as did my early experiences with high-vac lines and ruthenium chemistry under the

tutelage of then graduate student Steve Singer. The UW department remains a standard in my mind for a collegial chemistry atmosphere.

Several other people have contributed to the palladium(II) oxidation project: Eric Ferreira, Jeff Bagdanoff, Dr. Yeeman Ramtohul, David Ebner, Dan Caspi, Ryan McFadden, JT Mohr, Dr. Haiming Zhang, and Dr. Toyoki Nishimata. I thank Eric Ferreira for getting it all started, for his insightful comments, and for setting high standards. Simply put, he worked really hard, and his efforts have benefited numerous members of the group, including myself. The ever laid-back Dr. Yeeman Ramtohul came along at just the right time to help finish off the oxidative cyclization project before it drove me crazy. The efforts of Jeff Bagdanoff to develop the OKR beyond the initial results were essential to my own work – eventually the project was far enough along that Brian was willing to let me look into some mechanistic questions. Dan Caspi, Dave Ebner, and Ryan McFadden's contributions to the synthetic applications of the OKR were an essential phase of the project. Palladium oxidation chemistry lives on through the work of Dave Ebner and Dr. Toyoki Nishimata. Guys, maybe someday you will find another ligand besides sparteine...

When I first came to Caltech, the "original conditions" of 204 Church had a huge influence on my graduate career. It was an intense time in the lab, and the amount of work we got done during those early years is now almost inconceivable. In particular I would like to thank Jeremy May, Dr. Richmond Sarpong, and Uttam Tambar (even though Uttam ditched us for Crellin, he made up for it by many nights at Amigos) for their support and friendship over the years. I especially have to thank my baymate of four years, Neil Garg. Neil's chemistry skills, work ethic, thoughtfulness, and dedication have been inspiring throughout my time at Caltech and were a big influence in the early years. We had numerous great conversations about chemistry and everything else, which I miss a lot, but luckily he hasn't moved away from Pasadena yet and he and his wife Lindsey remain good friends. I thank him also for his assistance in thesis preparation. It will be fun to see his career develop.

Updated 204 Church shows much promise and has been very kind in tolerating my thesis writing insanity. Dr. Toyoki Nishimata has been a great baymate over the past year, not only due to his top-notch chemistry skills but also because of our highly amusing conversations about the English language. I'm sure he will be relieved when I finally clean the towering piles of papers off my desk. Dr. John Phillips holds

down the fort Badger-style, and it's great to have a true organometallic chemist in the lab, Nat Sherden, to keep the interest in metals alive. I thank everyone else in updated 204 Church for a calm and pleasant work environment.

Of the younger generations, there are a number of people I would like to acknowledge: Dan Caspi for late nights at Amigos, other party times, and his attention to detail – Caspi, your love for Vegas may be overshadowed only by your obsession with all things computerized; Mike Krout, JT Mohr and Caspi for entertaining lunchtime conversations over tacos; JT Mohr, Jenny Roizen, Mike Krout, Jenn Stockdill, Dave Ebner, Dan Caspi, and John Enquist for essential proofreading and general thesis-assembly assistance. It is exciting to see new generations enter the lab after the tumultuous early stages, and I wish you all the best...all the best TLC plates.

The Grubbs group has been kind enough to make me an honorary group member through many chemistry discussions, hallway parties, trips to the Ath, pub crawls, and general friendliness. Erin Guidry, Dr. Greg Beutner, Jacob Berlin, and Dr. Tobias Ritter have been good friends over the past few years. I thank Andy Hejl for lots of 500 NMR assistance during thesis crunch time. Drs. Jen Love and James Tsai provided helpful discussions and experimental advice in the early days. 130 Church, past and present, is a lab to be reckoned with, on or off the foosball table. I wish to also thank Professor Dan O'Leary, a visiting professor from Pomona College, for his NMR advice and for commiserating with me over sparteine chemistry.

The Bercaw group has been extremely important to me, scientifically and socially. Jon Owen asked many critical questions about my chemistry that influenced the direction of my projects, and has remained a great friend. I always appreciated his willingness to sit down and think about something, and to stay up way too late at Lucky Baldwin's. Jon, here's to doing something different as a postdoc. Susan Schofer has been a great friend over the past few years, despite moving to Sweden and back again. I miss all the crazy times we had at Amigos but I'm sure we will have many more once we both become world travelers. Lily Ackermann was a good friend during tough times, and I thank her for many helpful chemistry discussions. Dave "good times" Weinberg, Theo Agapie, and Jeff Byers, my classmates, you guys are crazy! I appreciate many hilarious discussions and especially Beer O'Clock. Theo, I have thoroughly enjoyed our

conversations over the past year and I'm sure you will survive the marathon long enough to buy my crappy car.

There are many other people to thank: Smith Nielsen of the Goddard lab for his willingness to do calculations on a complicated system and his continuing interest in sparteine-related chemistry; Connie Lu and Dr. Cora MacBeth of the Peters lab for experimental advice and electrochemistry assistance; the infamous Joel Austin of the DMAC lab; Rebecca Connor, Meghana Bhatt and Yen Nguyen for friendship; Jon Feenstra from the Zewail group for his intense interest in birds and willingness to share his knowledge; James Petersson, for first suggesting the name of my future postdoc advisor; and Caltech Women's Ultimate for a pleasant diversion. Special thanks also to our emeritus professors Dr. John D. Roberts, one of the giants of NMR, for attending my talks, and Dr. Nelson J. Leonard, without whose groundbreaking work in the synthesis of lupin alkaloids this thesis would not be the same. I thank Nelson also for several interesting discussions on this topic.

I wish to thank the wonderful support staff in the Chemistry department, who manage to make things run smoothly despite demands from all sides. Thanks to Rick Gerhart (for making me a Schlenk line!), Mike Roy, Joe Drew, Mo Renteria, Terry James, Steve Gould, Lillian Kremar, Lynne Martinez, Linda Syme, Chris Smith, and especially Dian Buchness, who helps hold this department together. I thank Mona Shagoli for her efforts in the mass spec facility. Tom Dunn is another person without whom the department could not function, and I thank him for his kindness during a tough experience. Larry Henling and Mike Day, our crystallographers, are unique in their willingness to have a look at even the crappiest crystals, and I thank them for solving all of my structures, even though they all contained sparteine. The NMR facility has gone though many ups and downs during my time at Caltech, and most of the ups are due to the terrific efforts of Scott Ross. Scott, I really enjoyed working with you to improve the facility, and I wish you all the best in the future.

I thank my family – my parents John and Beth Trend for their unwavering support and encouragement throughout life and during the tough times of graduate school, and my sister Alice, who, even from Indonesia, has given me essential support and friendship. I must also thank all of my non-Caltech friends who have patiently put up with my long work hours and general unavailability over the past five years. Your support has meant a lot to me.

Finally, I give my deepest appreciation to Andrew Waltman. Even from Switzerland he has been an essential part of my graduate career. Among many other things, his incisive questions, experimental advice and editorial assistance have helped make this thesis possible. My time at Caltech wouldn't have been nearly as good without you, Andy, and your constant love and support, critical thinking, comic relief and care for me have been so important to me over the past four years. I can't wait for our future adventures together.

ABSTRACT

Oxidation is one of the most fundamental and important processes in nature. It would be advantageous to chemically replicate the high substrate specificity and selectivity observed in oxidative enzymes. Several such synthetic processes have been developed that involve the transfer of a heteroatom to a substrate in an asymmetric fashion. Enantioselective oxidative dehydrogenations, which do not involve transfer of a heteroatom, are much less common. Reactions of this type have recently been developed for the oxidative kinetic resolution of secondary alcohols using palladium(II) catalysis, dioxygen, and the chiral ligand (–)-sparteine.

This general approach (palladium(II), dioxygen, ligand) was applied to the development of oxidative heteroatom/olefin cyclizations to form dihydrobenzofurans, cyclic ethers, lactones and lactams. The nonenantioselective reaction employs pyridine as a ligand. These conditions could be extended to the enantioselective cyclization of allyl-appended phenols through the use of (–)-sparteine as a ligand.

The mechanism of the oxidative heteroatom/olefin cyclizations was explored via stereospecifically deuterium-labeled substrates. These studies indicate that the stereochemistry of oxypalladation for primary alcohol substrates is syn, whether a mono- or bidentate ligand is used. In contrast, cyclizations of deuterium-labeled carboxylic acid substrates undergo anti oxypalladation.

The origins of stereoselectivity in the oxidative kinetic resolution of secondary alcohols using the C_1 symmetric ligand (–)-sparteine were investigated through structural and reactivity studies of a variety of ((–)-sparteine)palladium(II) complexes. A model for the observed selectivity was developed, and is supported by theoretical calculations. Experiments with the C_2 symmetric diastereomers of (–)-sparteine highlight the special properties of (–)-sparteine that make it a uniquely effective ligand in the kinetic resolution.

TABLE OF CONTENTS

Acknowledgements iii
Abstract viii
Table of Contents ix
List of Figures xiv
List of Schemes xxiii
List of Tables xxv
List of Abbreviations xxviii

Chapter 1 – Palladium(II)-Catalyzed Oxidase-Type Reactions

1.1 Introduction and background 1
1.2 Palladium(II) as a catalyst for enantioselective oxidase-type reactions 3
1.3 Notes and references 6

Chapter 2 – The Development of Palladium(II)-Catalyzed Oxidative Cyclizations in a Nonpolar Solvent Using Molecular Oxygen

2.1 Introduction and background 9
2.1.1 Introduction 9
2.1.2 Background 10
2.2 The development of nonenantioselective palladium(II)-catalyzed oxidative heteroatom/olefin cyclizations 16
2.2.1 The effect of palladium X^- ligand 16
2.2.2 The effect of exogenous base 17
2.2.3 The effect of the nitrogen-containing ligand 19
2.2.4 Cyclizations of *para*-substituted allyl-appended phenols 21
2.2.5 Cyclizations of multiply substituted allyl-appended phenols 21
2.2.6 Cyclizations of phenols with different olefin substitution patterns 22
2.2.7 Oxidative cyclizations of primary alcohols with olefins 23
2.2.8 Oxidative cyclizations of carboxylic acids and acid derivatives onto olefins 24
2.2.9 Reaction scope and limitations 25
2.3 The elaboration of the nonenantioselective conditions to an asymmetric version 26
2.3.1 Chiral ligand screen 26
2.3.2 Optimization of the asymmetric reaction – screen of palladium sources. 28
2.3.3 Optimization of the asymmetric reaction – effect of basic additives on the asymmetric oxidative cyclization 30
2.3.4 Enantioselective oxidative cyclization of phenol substrates 30
2.4 Proposed rationale for the observed stereochemistry 32
2.4.1 Rationale based on external nucleophilic attack 32

2.4.2 Rationale based on internal C–O bond formation 33

2.5 Conclusion 34

2.6 Experimental Section 35

2.6.1 Materials and Methods 35

2.6.2 General procedure for the oxidative cyclization of **26**. Palladium(II) source and additive optimization reactions shown in Tables 2.2.1 and 2.2.2 36

2.6.3 General procedure for the racemic oxidative cyclization of **26**. Ligand optimization reactions shown in Table 2.2.3 36

2.6.4 Preparation of $L_nPd(TFA)_2$ complexes 37

2.6.5 Synthesis of substituted phenols 45

2.6.6 General procedure for the racemic oxidative cyclization of phenols shown in Tables 2.2.4, 2.2.5, and 2.2.6 55

2.6.7 Synthesis of primary alcohol substrates 62

2.6.8 General procedure for the oxidative cyclizations of primary alcohols shown in Table 2.2.7 65

2.6.9 Synthesis of carboxylic acid and carboxylic acid derivative substrates 67

2.6.10 General procedure for the carboxylic acid and acid derivative oxidative cyclizations shown in Table 2.2.8 76

2.6.11 General procedure for asymmetric oxidative cyclization of **26**. Ligand screening trials shown in Table 2.3.1 82

2.6.12 General procedure for asymmetric oxidative cyclization of **26**. Palladium source and basic additive screening trials shown in Tables 2.3.2 and 2.3.3 82

2.6.13 The synthesis of (sp)$Pd(TFA)_2$ (**134**) 83

2.6.14 General procedure for the asymmetric oxidative cyclization of phenols shown in Table 2.3.4 84

2.6.15 Methods for the determination of % conversion and % enantiomeric excess in the asymmetric oxidative cyclization of phenols 86

2.6.16 General procedure for cyclization of **84** and attempted suppression of **135** as shown in Table 2.3.5 87

2.7 Notes and references 89

Appendix 2.1 Spectra Relevant to Chapter 2 95

Appendix 2.2 X-ray Crystallographic Data for (sp)$Pd(TFA)_2$ (**134**) 203

Chapter 3 – Mechanistic Investigations of Palladium(II)-Catalyzed Oxidative Cyclizations 215

3.1 Introduction and background 215

3.1.1 Introduction 215

3.1.2 Background 214

3.2 Mechanistic investigation of the oxidative cyclization of primary alcohols using deuterium-labeled substrates 220

3.2.1 Primary alcohol cyclizations of deuterium-labeled substrates with (pyridine)$_2$Pd(TFA)$_2$ (**144**) 220
3.2.2 Rationale for the product distribution from primary alcohol cyclizations of deuterium-labeled substrates with (pyridine)$_2$Pd(TFA)$_2$ (**144**) 224
3.2.3 Possibilities for reactive pathways involving palladium(IV) 225
3.2.4 Considerations regarding a π-allyl mechanism 227
3.2.5 The effect of chloride ion on the stereochemistry of oxypalladation 228
3.2.6 Deuterium-labeling studies of primary alcohol substrates in the presence of a bidentate ligand 229
3.2.7 Considerations regarding mono- and bidentate ligands in the oxidative cyclization of primary alcohols 230

3.3 Mechanistic investigations of the oxidative cyclization of carboxylic acids using deuterium-labeled substrates 232
3.4 Summary and conclusion 233

3.5 Experimental section 235
3.5.1 Materials and Methods 235
3.5.2 The preparation of deuterium-labeled primary alcohol substrates 236
3.5.3 Representative procedure for the cyclization of deuterium-labeled alcohol substrates ***trans*-3-*d*-212** and ***cis*-3-*d*-212**, and cyclohexene **212** shown in Scheme 3.2.2 242
3.5.4 Attempted cyclization of a terminal olefin-appended phenol as shown in Scheme 3.2.3 246
3.5.5 Cyclization of ***cis*-3-*d*-212** with (pyridine)$_2$PdCl$_2$ as shown in Scheme 3.2.4 247
3.5.6. Representative procedure for the cyclization of deuterium-labeled alcohol substrates ***trans*-3-*d*-212** and ***cis*-3-*d*-212** with (dipyridyl)Pd(TFA)$_2$ (**149**) and (sp)Pd(TFA)$_2$ (**134**) shown in Scheme 3.2.5 248
3.5.7 The preparation of deuterium-labeled carboxylic acid substrates **cis-3-d-242** and ***trans*-3-*d*-242** 250
3.5.8 Representative procedure for the cyclization of deuterium-labeled acid substrates **cis-3-d-242** and **trans-3-d-242** as shown in Scheme 3.3.1 253
3.6 Notes and references 256

Appendix 3.1 – Spectra Relevant to Chapter 3 261

Chapter 4 – Structural Features and Reactivity of (sp)PdCl$_2$: A Model for Selectivity in the Oxidative Kinetic Resolution of Secondary Alcohols 293

4.1 Introduction and background 293
4.1.1 Introduction 293
4.1.2 Background 294

4.2 Reactivity and structural studies of (–)-sparteine palladium complexes 299
4.2.1 The reactivity of (sp)PdCl$_2$ (**184**) with pyridine derivatives and their solid-state9structures 299

4.2.2 The synthesis and reactivity of a palladium alkoxide as a model for an intermediate in the oxidative kinetic resolution 305

4.3 An experimentally derived model for the stereoselectivty observed in the oxidative kinetic resolution 309

4.3.1 A description of the model 309

4.3.2 Calculations support the model 312

4.3.3 The potential effect of the halide ligand on selectivity and reactivity 313

4.4 The properties and reactivity of α- and β-isosparteine in the oxidative kinetic resolution 316

4.4.1 A structural comparison of the three sparteine diastereomers 316

4.4.2 (–)-α-Isosparteine as a ligand in the oxidative kinetic resolution 317

4.4.3 (+)-β-Isosparteine as a ligand in the oxidative kinetic resolution 320

4.4.4 Ligand substitution experiments with PPh_3 and the three (sparteine)$PdCl_2$ complexes 322

4.5 Summary and conclusion 326

4.6 Experimental section 327

4.6.1 Materials and Methods 327

4.6.2 The preparation of palladium complexes of pyridine derivatives and the reactions thereof 328

4.6.3 The preparation of palladium alkoxide complexes and the reactions thereof 332

4.6.4 The preparation of (sp)$PdBr_2$ (**288**) and reactions thereof 337

4.6.5 The preparation of sparteine ligands, their metal complexes, and the reactions thereof 339

4.7 Notes and references 350

Appendix 4.1 – Spectra Relevant to Chapter 4 355

Appendix 4.2 – X-ray Crystallographic Data for (sp)$PdCl_2$ (**184**) 379

Appendix 4.3 – X-ray Crystallographic Data for (sp)Pd(pyr)$Cl^+SbF_6^-$ (**257**) 387

Appendix 4.4 – X-ray Crystallographic Data for ((sp)$PdCl)_2^{2+}2SbF_6^-$ (**297**) 397

Appendix 4.5 – X-ray Crystallographic Data for (sp)Pd(2-methylisoquinoline)Cl^+SbF_6 (**260/261**) 403

Appendix 4.6 – X-ray Crystallographic Data for (sp)Pd(2-mesitypyridine)$Cl^+SbF_6^-$ (**265**) 417

Appendix 4.7 – X-ray Crystallographic Data for (sp)Pd($OCCF_3$Ph)Cl (**271**) 427

Appendix 4.8 – X-ray Crystallographic Data for (sp)Pd($OCCF_3Ph$)$_2$ (**274**) 439

Appendix 4.9 – X-ray Crystallographic Data for (sp)$PdBr_2$ (**288**) 449

Appendix 4.10 – X-ray Crystallographic Data for (α-isosp)$PdBr_2$ (**289**)..... 455

Appendix 4.11 – X-ray Crystallographic Data for (β-isosp)$PdBr_2$ (**290**) 463

Appendix 4.12 – Tabulation of Palladium Alkoxide Structures Possessing β-Hydrogens Reported in the Cambridge Structural Database.... 469

Appendix 5 – X-ray Crystallographic Data for (sp)Pd(pyridine)$TFA^+SbF_6^-$ (**312**)..... 471

Appendix 6 – Understanding Asymmetric Induction by C_1 Symmetric Ligands..... 479

Appendix 7 – Notebook Cross-Reference..... 491

Comprehensive Bibliography..... 495

Subject Index 507

LIST OF FIGURES

Chapter 1

Figure 1.1.1 Oxygenase and oxidase enzymes 2
Figure 1.1.2 Asymmetric oxygenase-type reactions 3
Figure 1.2.1 Potential asymmetric oxidase-type reactions 4
Figure 1.2.2 Palladium(II)-cataylzed oxidase-type reactions 5
Figure 1.2.3 Asymmetric palladium(II) catalyzed oxidase-type reactions 5

Chapter 2

Figure 2.1.1 Oxidative cyclization reactions 10
Figure 2.1.2 Uemura's proposed mechanism for the oxidation of secondary alcohols 14
Figure 2.1.3 A potential mechanism for the cyclization of heteroatoms with pendant olefins 16
Figure 2.4.1 Stereochemical rationale for external nucleophilic attack 33
Figure 2.4.2 Stereochemical rationale for internal C–O bond formation 34

Appendix 2.1

Figure A2.1.1 ^{1}H NMR spectrum (300 MHz, $CDCl_3$) of **26** 96
Figure A2.1.2 ^{13}C NMR spectrum (75 MHz, $CDCl_3$) of **26** 97
Figure A2.1.3 IR spectrum (thin film/NaCl) of **26** 97
Figure A2.1.4 ^{1}H NMR spectrum (300 MHz, $CDCl_3$) of **27** 98
Figure A2.1.5 ^{13}C NMR spectrum (75 MHz, $CDCl_3$) of **27** 99
Figure A2.1.6 IR spectrum (thin film/NaCl) of **27** 99
Figure A2.1.7 ^{1}H NMR spectrum (300 MHz, $CDCl_3$) of **80** 100
Figure A2.1.8 ^{13}C NMR spectrum (75 MHz, $CDCl_3$) of **80** 101
Figure A2.1.9 IR spectrum (thin film/NaCl) of **80** 101
Figure A2.1.10 ^{1}H NMR spectrum (300 MHz, $CDCl_3$) of **81** 102
Figure A2.1.11 ^{13}C NMR spectrum (75 MHz, $CDCl_3$) of **81** 103
Figure A2.1.12 IR spectrum (thin film/NaCl) of **81** 103
Figure A2.1.13 ^{1}H NMR spectrum (300 MHz, $CDCl_3$) of **82** 104
Figure A2.1.14 ^{13}C NMR spectrum (75 MHz, $CDCl_3$) of **82** 105
Figure A2.1.15 IR spectrum (thin film/NaCl) of **82** 105
Figure A2.1.16 ^{1}H NMR spectrum (300 MHz, $CDCl_3$) of **83** 106
Figure A2.1.17 ^{13}C NMR spectrum (75 MHz, $CDCl_3$) of **83** 107
Figure A2.1.18 IR spectrum (thin film/NaCl) of **83** 107
Figure A2.1.19 ^{1}H NMR spectrum (300 MHz, $CDCl_3$) of **84** 108
Figure A2.1.20 ^{13}C NMR spectrum (75 MHz, $CDCl_3$) of **84** 109
Figure A2.1.21 IR spectrum (thin film/NaCl) of **84** 109
Figure A2.1.22 ^{1}H NMR spectrum (300 MHz, $CDCl_3$) of **85** 110
Figure A2.1.23 ^{13}C NMR spectrum (75 MHz, $CDCl_3$) of **85** 111

Figure A2.1.24 IR spectrum (thin film/NaCl) of **85**.....111
Figure A2.1.25 ^{1}H NMR spectrum (300 MHz, $CDCl_3$) of **86**.....112
Figure A2.1.26 ^{13}C NMR spectrum (75 MHz, $CDCl_3$) of **86**.....113
Figure A2.1.27 IR spectrum (thin film/NaCl) of **86**.....113
Figure A2.1.28 ^{1}H NMR spectrum (300 MHz, $CDCl_3$) of **87**.....114
Figure A2.1.29 ^{13}C NMR spectrum (75 MHz, $CDCl_3$) of **87**.....115
Figure A2.1.30 IR spectrum (thin film/NaCl) of **87**.....115
Figure A2.1.31 ^{1}H NMR spectrum (300 MHz, $CDCl_3$) of **88**.....116
Figure A2.1.32 ^{13}C NMR spectrum (75 MHz, $CDCl_3$) of **88**.....117
Figure A2.1.33 IR spectrum (thin film/NaCl) of **88**.....117
Figure A2.1.34 ^{1}H NMR spectrum (300 MHz, $CDCl_3$) of **89**.....118
Figure A2.1.35 ^{13}C NMR spectrum (75 MHz, $CDCl_3$) of **89**.....119
Figure A2.1.36 IR spectrum (thin film/NaCl) of **89**.....119
Figure A2.1.37 ^{1}H NMR spectrum (300 MHz, $CDCl_3$) of **90**.....120
Figure A2.1.38 ^{13}C NMR spectrum (75 MHz, $CDCl_3$) of **90**.....121
Figure A2.1.39 IR spectrum (thin film/NaCl) of **90**.....121
Figure A2.1.40 ^{1}H NMR spectrum (300 MHz, $CDCl_3$) of **91**.....122
Figure A2.1.41 ^{13}C NMR spectrum (75 MHz, $CDCl_3$) of **91**.....123
Figure A2.1.42 IR spectrum (thin film/NaCl) of **91**.....123
Figure A2.1.43 ^{1}H NMR spectrum (300 MHz, $CDCl_3$) of **92**.....124
Figure A2.1.44 ^{13}C NMR spectrum (75 MHz, $CDCl_3$) of **92**.....125
Figure A2.1.45 IR spectrum (thin film/NaCl) of **92**.....125
Figure A2.1.46 ^{1}H NMR spectrum (300 MHz, $CDCl_3$) of **93**.....126
Figure A2.1.47 ^{13}C NMR spectrum (75 MHz, $CDCl_3$) of **93**.....127
Figure A2.1.48 IR spectrum (thin film/NaCl) of **93**.....127
Figure A2.1.49 ^{1}H NMR spectrum (300 MHz, $CDCl_3$) of **94**.....128
Figure A2.1.50 ^{13}C NMR spectrum (75 MHz, $CDCl_3$) of **94**.....129
Figure A2.1.51 IR spectrum (thin film/NaCl) of **94**.....129
Figure A2.1.52 ^{1}H NMR spectrum (300 MHz, $CDCl_3$) of **95**.....130
Figure A2.1.53 ^{13}C NMR spectrum (75 MHz, $CDCl_3$) of **95**.....131
Figure A2.1.54 IR spectrum (thin film/NaCl) of **95**.....131
Figure A2.1.55 ^{1}H NMR spectrum (300 MHz, $CDCl_3$) of **96**.....132
Figure A2.1.56 ^{13}C NMR spectrum (75 MHz, $CDCl_3$) of **96**.....133
Figure A2.1.57 IR spectrum (thin film/NaCl) of **96**.....133
Figure A2.1.58 ^{1}H NMR spectrum (300 MHz, $CDCl_3$) of **97**.....134
Figure A2.1.59 ^{13}C NMR spectrum (75 MHz, $CDCl_3$) of **97**.....135
Figure A2.1.60 IR spectrum (thin film/NaCl) of **97**.....135
Figure A2.1.61 ^{1}H NMR spectrum (300 MHz, $CDCl_3$) of **98**.....136
Figure A2.1.62 ^{13}C NMR spectrum (75 MHz, $CDCl_3$) of **98**.....137
Figure A2.1.63 IR spectrum (thin film/NaCl) of **98**.....137
Figure A2.1.64 ^{1}H NMR spectrum (300 MHz, $CDCl_3$) of **99**.....138
Figure A2.1.65 ^{13}C NMR spectrum (75 MHz, $CDCl_3$) of **99**.....139

Figure A2.1.66 IR spectrum (thin film/NaCl) of **99**.....139
Figure A2.1.67 ^{1}H NMR spectrum (300 MHz, $CDCl_3$) of **45**.....140
Figure A2.1.68 ^{13}C NMR spectrum (75 MHz, $CDCl_3$) of **45**.....141
Figure A2.1.69 IR spectrum (thin film/NaCl) of **45**.....141
Figure A2.1.70 ^{1}H NMR spectrum (300 MHz, $CDCl_3$) of **47**.....142
Figure A2.71 ^{13}C NMR spectrum (75 MHz, $CDCl_3$) of **47**.....143
Figure A2.1.72 IR spectrum (thin film/NaCl) of **47**.....143
Figure A2.1.73 ^{1}H NMR spectrum (300 MHz, $CDCl_3$) of **28**.....144
Figure A2.1.74 ^{13}C NMR spectrum (75 MHz, $CDCl_3$) of **28**.....145
Figure A2.1.75 IR spectrum (thin film/NaCl) of **28**.....145
Figure A2.1.76 ^{1}H NMR spectrum (300 MHz, $CDCl_3$) of **29**.....146
Figure A2.1.77 ^{13}C NMR spectrum (75 MHz, $CDCl_3$) of **29**.....147
Figure A2.1.78 IR spectrum (thin film/NaCl) of **29**.....147
Figure A2.1.79 ^{1}H NMR spectrum (300 MHz, $CDCl_3$) of **100**.....148
Figure A2.1.80 ^{13}C NMR spectrum (75 MHz, $CDCl_3$) of **100**.....149
Figure A2.1.81 IR spectrum (thin film/NaCl) of **100**.....149
Figure A2.1.82 ^{1}H NMR spectrum (300 MHz, $CDCl_3$) of **101**.....150
Figure A2.1.83 ^{13}C NMR spectrum (75 MHz, $CDCl_3$) of **101**.....151
Figure A2.1.84 IR spectrum (thin film/NaCl) of **101**.....151
Figure A2.1.85 ^{1}H NMR spectrum (300 MHz, $CDCl_3$) of **102**.....152
Figure A2.1.86 ^{13}C NMR spectrum (75 MHz, $CDCl_3$) of **102**.....153
Figure A2.1.87 IR spectrum (thin film/NaCl) of **102**.....153
Figure A2.1.88 ^{1}H NMR spectrum (300 MHz, $CDCl_3$) of **104**.....154
Figure A2.1.89 ^{13}C NMR spectrum (75 MHz, $CDCl_3$) of **104**.....155
Figure A2.1.90 IR spectrum (thin film/NaCl) of **104**.....155
Figure A2.1.91 ^{1}H NMR spectrum (300 MHz, $CDCl_3$) of **107**.....156
Figure A2.1.92 ^{13}C NMR spectrum (75 MHz, $CDCl_3$) of **107**.....157
Figure A2.1.93 IR spectrum (thin film/NaCl) of **107**.....157
Figure A2.1.94 ^{1}H NMR spectrum (300 MHz, $CDCl_3$) of **109**.....158
Figure A2.1.95 ^{13}C NMR spectrum (75 MHz, $CDCl_3$) of **109**.....159
Figure A2.1.96 IR spectrum (thin film/NaCl) of **109**.....159
Figure A2.1.97 ^{1}H NMR spectrum (300 MHz, $CDCl_3$) of **110**.....160
Figure A2.1.98 ^{13}C NMR spectrum (75 MHz, $CDCl_3$) of **110**.....161
Figure A2.1.99 IR spectrum (thin film/NaCl) of **110**.....161
Figure A2.1.100 ^{1}H NMR spectrum (300 MHz, $CDCl_3$) of **111**.....162
Figure A2.1.101 ^{13}C NMR spectrum (75 MHz, $CDCl_3$) of **111**.....163
Figure A2.1.102 IR spectrum (thin film/NaCl) of **111**.....163
Figure A2.1.103 ^{1}H NMR spectrum (300 MHz, $CDCl_3$) of **113**.....164
Figure A2.1.104 ^{13}C NMR spectrum (75 MHz, $CDCl_3$) of **113**.....165
Figure A2.1.105 IR spectrum (thin film/NaCl) of **113**.....165
Figure A2.1.106 ^{1}H NMR spectrum (300 MHz, $CDCl_3$) of **112**.....166
Figure A2.1.107 ^{13}C NMR spectrum (75 MHz, $CDCl_3$) of **112**.....167

Figure A2.1.108 IR spectrum (thin film/NaCl) of **112** 167
Figure A2.1.109 ^{1}H NMR spectrum (300 MHz, $CDCl_3$) of **114** 168
Figure A2.1.110 ^{13}C NMR spectrum (75 MHz, $CDCl_3$) of **114** 169
Figure A2.1.111 IR spectrum (thin film/NaCl) of **114** 169
Figure A2.1.112 ^{1}H NMR spectrum (300 MHz, acetone-d_6) of **115** 170
Figure A2.1.113 ^{13}C NMR spectrum (75 MHz, acetone-d_6) of **115** 171
Figure A2.1.114 IR spectrum (thin film/NaCl) of **115** 171
Figure A2.1.115 ^{1}H NMR spectrum (300 MHz, acetone-d_6) of **116a** 172
Figure A2.1.116 ^{13}C NMR spectrum (75 MHz, acetone-d_6) of **116a** 173
Figure A2.1.117 IR spectrum (thin film/NaCl) of **116a** 173
Figure A2.1.118 ^{1}H NMR spectrum (300 MHz, acetone-d_6) of **116b** 174
Figure A2.1.119 ^{13}C NMR spectrum (75 MHz, acetone-d_6) of **116b** 175
Figure A2.1.120 IR spectrum (thin film/NaCl) of **116b** 175
Figure A2.1.121 ^{1}H NMR spectrum (300 MHz, $CDCl_3$) of **117** 176
Figure A2.1.122 ^{13}C NMR spectrum (75 MHz, $CDCl_3$) of **117** 177
Figure A2.1.123 IR spectrum (thin film/NaCl) of **117** 177
Figure A2.1.124 ^{1}H NMR spectrum (300 MHz, $CDCl_3$) of **118** 178
Figure A2.1.125 ^{13}C NMR spectrum (75 MHz, $CDCl_3$) of **118** 179
Figure A2.1.126 IR spectrum (thin film/NaCl) of **118** 179
Figure A2.1.127 ^{1}H NMR spectrum (300 MHz, $CDCl_3$) of **134** 180
Figure A2.1.128 ^{13}C NMR spectrum (75 MHz, $CDCl_3$) of **134** 181
Figure A2.1.129 ^{1}H NMR spectrum (300 MHz, $CDCl_3$) of **135** 182
Figure A2.1.130 ^{13}C NMR spectrum (75 MHz, $CDCl_3$) of **135** 183
Figure A2.1.131 IR spectrum (thin film/NaCl) of **135** 183
Figure A2.1.132 ^{1}H NMR spectrum (300 MHz, $CDCl_3$) of **144** 184
Figure A2.1.133 ^{13}C NMR spectrum (75 MHz, $CDCl_3$) of **144** 185
Figure A2.1.134 ^{1}H NMR spectrum (300 MHz, $CDCl_3$) of **145** 186
Figure A2.1.135 ^{13}C NMR spectrum (75 MHz, $CDCl_3$) of **145** 187
Figure A2.1.136 ^{1}H NMR spectrum (300 MHz, $CDCl_3$) of **146** 188
Figure A2.1.137 ^{13}C NMR spectrum (75 MHz, $CDCl_3$) of **146** 189
Figure A2.1.138 ^{1}H NMR spectrum (300 MHz, $CDCl_3$) of **147** 190
Figure A2.1.139 ^{13}C NMR spectrum (75 MHz, $CDCl_3$) of **147** 191
Figure A2.1.140 ^{1}H NMR spectrum (300 MHz, $CDCl_3$) of **148** 192
Figure A2.1.141 ^{13}C NMR spectrum (75 MHz, $CDCl_3$) of **148** 193
Figure A2.1.142 ^{1}H NMR spectrum (300 MHz, $CDCl_3$) of **151** 194
Figure A2.1.143 ^{13}C NMR spectrum (75 MHz, $CDCl_3$) of **151** 195
Figure A2.1.144 ^{1}H NMR spectrum (300 MHz, $CDCl_3$) of **152** 196
Figure A2.1.145 ^{13}C NMR spectrum (75 MHz, $CDCl_3$) of **152** 197
Figure A2.1.146 ^{1}H NMR spectrum (300 MHz, CD_3OD) of **153** 198
Figure A2.1.147 ^{13}C NMR spectrum (75 MHz, CD_3OD) of **153** 199
Figure A2.1.148 ^{1}H NMR spectrum (300 MHz, CD_2Cl_2) of **154** 200
Figure A2.1.149 ^{13}C NMR spectrum (75 MHz, CD_2Cl_2) of **154** 201

Appendix 2.2

Figure A2.2.1 (sp)Pd(TFA)$_2$ (**134**) 203
Figure A2.2.2 Molecule A of (sp)Pd(TFA)$_2$ (**134**) showing trans orientation of the carboxyl oxygen atoms 206
Figure A2.2.3 Molecule B of (sp)Pd(TFA)$_2$ (**134**) showing cis orientation of the carboxyl oxygen atoms 207
Figure A2.2.4 Unit cell contents of (sp)Pd(TFA)$_2$ (**134**) 208
Figure A2.2.5 Stereo view of unit cell contents of (sp)Pd(TFA)$_2$ (**134**) 208

Chapter 3

Figure 3.1.1 Anti oxypalladation 216
Figure 3.1.2 Syn oxypalladation 217
Figure 3.1.3 Frontier orbitals of the cis migration of an olefin in a palladium complex 219
Figure 3.2.1 Coupling constant and NOE interactions for **214**. 224
Figure 3.2.2 Mechanistic rationale for the observed product distribution 225
Figure 3.2.3 Possible intermediates for a mechanism involving palladium(IV) 226
Figure 3.2.4 Comparison of reaction pathways with a monodentate and bidentate ligand 231
Figure 3.5.1 Comparison ^{1}H NMR spectrum of alcohol substrates 242
Figure 3.5.2 NOE analysis of cyclohexene **214** 244
Figure 3.5.3 Homodecoupling analysis of **cis-2-d-214** 245
Figure 3.5.4 ^{1}H NMR comparison spectrum of cyclized products 245

Appendix 3.1

Figure A3.1.1 ^{1}H NMR spectrum (500 MHz, $CDCl_3$) of ***cis-d*-210** 262
Figure A3.1.2 ^{13}C NMR spectrum (125 MHz, $CDCl_3$) of ***cis-d*-210** 263
Figure A3.1.3 ^{2}H NMR spectrum (76 MHz, $CHCl_3$) of ***cis-d*-210** 263
Figure A3.1.4 ^{1}H NMR spectrum (500 MHz, $CDCl_3$) of ***trans*-3-*d*-212** 264
Figure A3.1.5 ^{13}C NMR spectrum (125 MHz, $CDCl_3$) of ***trans*-3-*d*-212** 265
Figure A3.1.6 ^{2}H NMR spectrum (76 MHz, $CHCl_3$) of ***trans*-3-*d*-212** 265
Figure A3.1.7 ^{1}H NMR spectrum (500 MHz, $CDCl_3$) of ***cis*-3-*d*-212** 266
Figure A3.1.8 ^{13}C NMR spectrum (125 MHz, $CDCl_3$) of ***cis*-3-*d*-212** 267
Figure A3.1.9 ^{2}H NMR spectrum (76 MHz, $CHCl_3$of ***cis*-3-*d*-212** 267
Figure A3.1.10 ^{1}H NMR spectrum (500 MHz, $CDCl_3$) of **212** 268
Figure A3.1.11 ^{13}C NMR spectrum (125 MHz, $CDCl_3$) of **212** 269
Figure A3.1.12 IR spectrum (thin film/NaCl)) of **212** 269
Figure A3.1.13 ^{1}H NMR spectrum (500 MHz, $CDCl_3$) of **213** 270
Figure A3.1.14 ^{13}C NMR spectrum (125 MHz, $CDCl_3$) of **213** 271
Figure A3.1.15 IR spectrum (thin film/NaCl)) of **213** 271
Figure A3.1.16 ^{1}H NMR spectrum (500 MHz, $CDCl_3$) of ***cis*-2-*d*-214**, homodecoupling at 3.17, 3.87, 5.94, and 6.1 ppm (from bottom to top) 272
Figure A3.1.17 ^{1}H NMR spectrum (500 MHz, $CDCl_3$) of **214**, the minor component is **213** 273

Figure A3.1.18 ^{13}C NMR spectrum (125 MHz, $CDCl_3$) of **214**, the minor component is **213** 274
Figure A3.1.19 IR spectrum (thin film/NaCl)) of **214** in a mixture with **213** 274
Figure A3.1.20 ^{1}H NMR spectrum (500 MHz, $CDCl_3$) of **214** in a mixture with **213**. CycleNOE experiment with irradiation at 2.14 ppm 275
Figure A3.1.21 ^{1}H NMR spectrum (300 MHz, $CDCl_3$) of **3-*d*-213** and **3-*d*-214** 276
Figure A3.1.22 ^{2}H NMR spectrum (76 MHz, $CHCl_3$) of **3-*d*-213** and **3-*d*-214** 277
Figure A3.1.23 ^{2}H NMR spectrum (76 MHz, $CHCl_3$) of **213** and ***cis*-2-*d*-214** 277
Figure A3.1.24 ^{1}H NMR spectrum (500 MHz, $CDCl_3$) of **213** and ***cis*-2-*d*-214** 278
Figure A3.1.25 ^{1}H NMR spectrum (500 MHz, $CDCl_3$) of ***cis*-3-*d*-233** 279
Figure A3.1.26 ^{13}C NMR spectrum (125 MHz, $CDCl_3$) of ***cis*-3-*d*-233** 280
Figure A3.1.27 ^{2}H NMR spectrum (76 MHz, $CHCl_3$) of ***cis*-3-*d*-233** 280
Figure A3.1.28 ^{1}H NMR spectrum (500 MHz, $CDCl_3$) of ***trans*-3-*d*-233** 281
Figure A3.1.29 ^{13}C NMR spectrum (125 MHz, $CDCl_3$) of ***trans*-3-*d*-233** 282
Figure A3.1.30 ^{2}H NMR spectrum (76 MHz, $CHCl_3$) of ***trans*-3-*d*-233** 282
Figure A3.1.31 ^{1}H NMR spectrum (500 MHz, $CDCl_3$) of **233** 283
Figure A3.1.32 ^{13}C NMR spectrum (125 MHz, $CDCl_3$) of **233** 284
Figure A3.1.33 IR spectrum (thin film/NaCl)) of **233** 284
Figure A3.1.34 ^{1}H NMR spectrum (500 MHz, $CDCl_3$) of ***cis*-3-*d*-242** 285
Figure A3.1.35 ^{13}C NMR spectrum (125 MHz, $CDCl_3$) of ***cis*-3-*d*-242** 286
Figure A3.1.36 IR spectrum (thin film/NaCl)) of ***cis*-3-*d*-242** 286
Figure A3.1.37 ^{1}H NMR spectrum (500 MHz, $CDCl_3$) of ***trans*-3-*d*-242** 287
Figure A3.1.38 ^{13}C NMR spectrum (125 MHz, $CDCl_3$) of ***trans*-3-*d*-242** 288
Figure A3.1.39 ^{2}H NMR spectrum (76 MHz, $CHCl_3$ of ***trans*-3-*d*-242** 288
Figure A3.1.40 ^{1}H NMR spectrum (500 MHz, $CDCl_3$) of **243** 289
Figure A3.1.41 ^{13}C NMR spectrum (125 MHz, $CDCl_3$) of **243** 290
Figure A3.1.42 IR spectrum (thin film/NaCl)) of **243** 290
Figure A3.1.43 ^{1}H NMR spectrum (300 MHz, $CDCl_3$) of **3-*d*-243** 291
Figure A3.1.44 ^{13}C NMR spectrum (125 MHz, $CDCl_3$) of **3-*d*-243** 292
Figure A3.1.45 ^{2}H NMR spectrum (76 MHz, $CHCl_3$) of **3-*d*-243** 292

Chapter 4

Figure 4.1.1 Alcohol oxidation by palladium 296
Figure 4.1.2 (sp)$PdCl_2$ (**184**) 298
Figure 4.1.3 β-Hydrogen elimination with a C_2 symmetric ligand 299
Figure 4.2.1 ^{1}H NMR spectra for **265** 304
Figure 4.2.2 Quadrant diagram for (sp)Pd 304
Figure 4.2.3 Rationale for a stable palladium alkoxide 305
Figure 4.3.1 Model for selectivity in the oxidative kinetic resolution of secondary alcohols 310
Figure 4.3.2 Possibilities for β-hydrogen elimination 311
Figure 4.3.3 Theoretical model for the oxidative kinetic resolution of secondary alcohols 313

Figure 4.4.1 Comparison of the three sparteine diastereomers 317
Figure 4.4.2 Theoretical study of the conformations of **22**, **255**, and **256** 323
Figure 4.6.1 ^{1}H NMR spectra of **257** at +45 °C, +25 °C and with 1 equiv added pyridine 330
Figure 4.6.2 Reaction of **184** and PPh_3 observed by ^{1}H NMR 347
Figure 4.6.3 Reaction of **290** with PPh_3 observed by ^{1}H NMR 348
Figure 4.6.4 Reaction of **289** with PPh_3 observed by ^{31}P NMR 349

Appendix 4.1

Figure A4.1.1 ^{1}H NMR spectrum (500 MHz, acetone-d_6) of **257** 356
Figure A4.1.2 ^{13}C NMR spectrum (125 MHz, acetone-d_6) of **257** 357
Figure A4.1.3 ^{1}H NMR spectrum (500 MHz, acetone-d_6) of **260/261** 358
Figure A4.1.4 ^{13}C NMR spectrum (75 MHz, $CDCl_3$) of **260/261** 359
Figure A4.1.4 ^{1}H NMR spectrum (500 MHz, acetone-d_6) of **265** 360
Figure A4.1.5 ^{13}C NMR spectrum (75 MHz, $CDCl_3$) of **265** 361
Figure A4.1.6 ^{1}H NMR spectrum (300 MHz, CD_2Cl_2) of **271** 362
Figure A4.1.7 ^{13}C NMR spectrum (75 MHz, CD_2Cl_2) of **271** 363
Figure A4.1.8 ^{19}F NMR spectrum (282 MHz, CD_2Cl_2) of **271** 363
Figure A4.1.9 ^{1}H NMR spectrum (300 MHz, CD_2Cl_2) of **274** 364
Figure A4.1.10 ^{13}C NMR spectrum (125 MHz, CD_2Cl_2) of **274** 365
Figure A4.1.11 ^{19}F NMR spectrum (282 MHz, CD_2Cl_2) of **274** 365
Figure A4.1.12 ^{1}H NMR spectrum (300 MHz, $CDCl_3$) of **288** 366
Figure A4.1.13 ^{13}C NMR spectrum (75 MHz, $CDCl_3$) of **288** 367
Figure A4.1.14 ^{1}H NMR spectrum (500 MHz, benzene-d_6) of **293** 368
Figure A4.1.15 ^{13}C NMR spectrum (125 MHz, $CDCl_3$) of **293** 369
Figure A4.1.16 IR spectrum (thin film/NaCl)) of **293** 369
Figure A4.1.17 ^{1}H NMR spectrum (500 MHz, benzene-d_6) of **255** 370
Figure A4.1.18 ^{13}C NMR spectrum (125 MHz, benzene-d_6) of **255** 371
Figure A4.1.19 IR spectrum (thin film/NaCl)) of **255** 371
Figure A4.1.20 ^{1}H NMR spectrum (300 MHz, CD_2Cl_2) of **289** 372
Figure A4.1.21 ^{13}C NMR spectrum (75 MHz, CD_2Cl_2) of **289** 373
Figure A4.1.22 ^{1}H NMR spectrum (300 MHz, $CDCl_3$) of **256** 374
Figure A4.1.23 ^{13}C NMR spectrum (125 MHz, $CDCl_3$) of **256** 375
Figure A4.1.24 IR spectrum (thin film/NaCl)) of **256** 375
Figure A4.1.25 ^{1}H NMR spectrum (500 MHz, $CDCl_3$) of **290** 376
Figure A4.1.26 ^{13}C NMR spectrum (125 MHz, $CDCl_3$) of **290** 377

Appendix 4.2

Figure A4.2.1 (sp)$PdCl_2$ (**184**) 379
Figure A4.2.2 Molecule **184** 381
Figure A4.2.3 Unit cell contents of **184** 382
Figure A4.2.4 Stereo view of unit cell contents of **184** 382

Appendix 4.3

Figure A4.3.1 (sp)Pd(pyr)$Cl^{+}SbF_6^{-}$ (**257**) 387
Figure A4.3.2 Molecule A of **257** 389
Figure A4.3.3 Molecule B of **257** 390
Figure A4.3.4 Unit cell contents of **257** 391
Figure A4.3.4 Stereo view of unit cell contents of **257** 391

Appendix 4.4

Figure A4.4.1 $((sp)PdCl)_2)^{2+}2SbF_6^{-}$ (**297**) 397
Figure A4.4.2 Molecule of **297** 399
Figure A4.4.3 Unit cell contents of **297** 400
Figure A4.4.4 Stereo view of unit cell contents of **297** 400

Appendix 4.5

Figure A4.5.1 (sp)Pd(2-methylisoquinoline)$Cl^{+}SbF_6^{-}$ (**260/261**) 401
Figure A4.5.2 Molecule A of **260/261** showing the disorder in the isoquinoline ligand 406
Figure A4.5.3 Molecule A of **260/261** showing the disorder modeled isotropically in one orientation of the isoquinoline ligand 407
Figure A4.5.4 Molecule A of **260/261** showing the disorder modeled isotropically in another orientation of the isoquinoline ligand, related to the first by 180° .. 408
Figure A4.5.5 Molecule B of **260/261** 409
Figure A4.5.6 Unit cell contents of **260/261** 410
Figure A4.5.7 Stereo view of unit cell contents of **260/261** 410

Appendix 4.6

Figure A4.6.1 (sp)Pd(2-mesitylpyridine)$Cl^{+}SbF_6^{-}$ (**265**) 417
Figure A4.6.2 Molecule of **265** 420
Figure A4.6.3 Unit cell contents of **265** 421
Figure A4.6.4 Stereo view of unit cell contents of **265** 421

Appendix 4.7

Figure A4.7.1 (sp)Pd($OCCF_3$Ph)Cl (**271**) 427
Figure A4.7.2 Molecule A of **271** 429
Figure A4.7.3 Molecule B of **271** 431
Figure A4.7.4 Overlay of molecules A and B of **271** 432
Figure A4.7.5 Unit cell contents of **271** 433
Figure A4.7.6 Stereo view of unit cell contents of **271** 433

Appendix 4.8

Figure A4.8.1 (sp)Pd($OCCF_3Ph)_2$ (**274**) 439
Figure A4.8.2 Molecule of **274** 442
Figure A4.8.3 Unit cell contents of **274** 443
Figure A4.8.4 Stereo view of unit cell contents of **274** 443

Appendix 4.9

Figure A.4.9.1 (sp)$PdBr_2$ (**288**) 449
Figure A4.9.2 Molecule of **288** 451
Figure A4.9.3 Unit cell contents of **288** 452
Figure A.4.9.4 Stereo view of unit cell contents of **288** 452

Appendix 4.10

Figure A4.10.1 (α-isosp)$PdCl_2$ (**289**) 455
Figure A4.10.2 Molecule of **289** 457
Figure A4.10.3 Unit cell contents of **289** 458
Figure A4.10.4 Stereo view of unit cell contents of **289** 458

Appendix 4.11

Figure A4.11.1 (β-isosp)$PdCl_2$ (**290**) 463
Figure A4.11.2 Molecule of **290** 464
Figure A4.11.3 Unit cell contents of **290** 465
Figure A4.11.4 Stereo view of unit cell contents of **290** 465

Appendix 5

Figure A5.1 (sp)Pd(pyridine)$TFA^+SbF_6^-$ (**312**) 471
Figure A5.2 Molecule of **312** 473
Figure A5.3 Unit cell contents of **312** 474
Figure A5.4 Stereo view of unit cell contents of **312** 474

Appendix 6

Figure A6.1 Common C_2 symmetric ligand scaffolds 480
Figure A6.2 Possible controlling factors for C_1 symmetric ligands 481
Figure A6.3 Phosphinooxazoline, or Pfaltz, ligand; nucleophilic attack at either allylic terminus 481
Figure A6.4 Model for asymmetric induction with the phosphinooxazole ligand framework 482
Figure A6.5 Mikami's model of asymmetric induction 483
Figure A6.6 Intricacies of cyclopropanation directed by a C_1 symmetric ligand in the Aratani process 486
Figure A6.7 Ohashi's P-chirogenic ligands 486

LIST OF SCHEMES

Chapter 2

Scheme 2.1.1 10
Scheme 2.1.2 11
Scheme 2.1.3 13
Scheme 2.1.4 13
Scheme 2.1.5 15

Chapter 3

Scheme 3.1.1 217
Scheme 3.1.2 218
Scheme 3.1.3 218
Scheme 3.1.4 220
Scheme 3.2.1 221
Scheme 3.2.2 223
Scheme 3.2.3 227
Scheme 3.2.4 228
Scheme 3.2.5 230
Scheme 3.3.1 233
Scheme 3.5.1 236

Chapter 4

Scheme 4.1.1 294
Scheme 4.2.1 300
Scheme 4.2.2 301
Scheme 4.2.3 302
Scheme 4.2.4 303
Scheme 4.2.5 306
Scheme 4.2.6 307
Scheme 4.2.7 308
Scheme 4.3.1 315
Scheme 4.4.1 318
Scheme 4.4.2 320
Scheme 4.4.3 324
Scheme 4.4.4 325

Appendix 4.4

Scheme A4.4.1 397

Appendix 6

Scheme A6.1 483
Scheme A6.2 484
Scheme A6.3 485
Scheme A6.4 487

LIST OF TABLES

Chapter 2

Table 2.2.1 Optimization of palladium(II) source 17
Table 2.2.2 Optimization of basic additive 18
Table 2.2.3 Oxidative cyclizations with substituted pyridyl and alkyl amine ligands 20
Table 2.2.4 Oxidative cyclizations of phenols with para substitution 21
Table 2.2.5 Oxidative cyclizations of multiply substituted phenols 22
Table 2.2.6 Oxidative cyclizations of phenols with different olefin substitution patterns 23
Table 2.2.7 Oxidative cyclization of primary alcohols with pendant olefins 24
Table 2.2.8 Oxidative cyclization of carboxylic acids and carboxylic acid derivatives 25
Table 2.3.1 Chiral ligand screen for the oxidative cyclization of **26** 28
Table 2.3.2 Optimization of palladium source for the asymmetric oxidative cyclization of **26** 29
Table 2.3.3 Basic additives in the asymmetric oxidative cyclization of **26** 30
Table 2.3.4 Enantioselective cyclization of olefin-appended phenols 31
Table 2.3.5 Attempted suppression of dimerization of **84** 32
Table 2.6.1 Methods employed for the determination of % conversion and % enantiomeric excess 86

Appendix 2.2

Table A2.2.1 Atomic coordinates for **134** (CCDC 192101) 209
Table A2.2.2 Selected bond lengths [Å] and angles [°] for **134** (CCDC 192101) 210
Table A2.2.3 Bond lengths [Å] and angles [°] for **134** (CCDC 192101) 210

Chapter 4

Table 4.1.1 Oxidative kinetic resolution of secondary alcohols 295
Table 4.3.1 A comparison of bond angles in (sp)Pd complexes 314
Table 4.3.2 Oxidative kinetic resolution with (sp)$PdBr_2$ (**288**) 315
Table 4.4.1 Oxidative kinetic resolution with (α-isosp)$PdCl_2$ (**289**) 318
Table 4.4.2 Oxidative kinetic resolution with (α-isosp)$PdCl_2$ (**289**) and Cs_2CO_3 319
Table 4.4.3 Oxidative kinetic resolution with (β-isosp)$PdCl_2$ (**290**) 321

Appendix 4.2

Table A4.2.1 Atomic coordinates for **184** (CCDC 203513) 383
Table A4.2.2 Selected bond lengths [Å] and angles [°] for **184** (CCDC 203513) 384
Table A4.2.3 Bond lengths [Å] and angles [°] for **184** (CCDC 203513) 384

Appendix 4.3

Table A4.3.1 Atomic coordinates for **257** (CCDC 213927) 392

Table A4.3.2 Bond lengths [Å] and angles [°] for **257** (CCDC 213927) 393

Appendix 4.4

Table A4.4.1 Atomic coordinates for **297** (CCDC 214435) 401
Table A4.4.2 Bond lengths [Å] and angles [°] for **297** (CCDC 214435) 401

Appendix 4.5

Table A4.5.1 Atomic coordinates for **260/261** (CCDC 217276..... 411
Table A4.5.2 Bond lengths [Å] and angles [°] for **260/261** (CCDC 217276)..... 413

Appendix 4.6

Table A4.6.1 Atomic coordinates for **265** (CCDC 215758) 422
Table A4.6.2 Selected bond lengths [Å] and angles [°] for **265** (CCDC 215758) 423
Table A4.6.3 Bond lengths [Å] and angles [°] for **265** (CCDC 215758) 423

Appendix 4.7

Table A4.7.1 Atomic coordinates for **271** (CCDC 222289) 432
Table A4.7.2 Selected bond lengths [Å] and angles [°] for **271** (CCDC 222289) 434
Table A4.7.3 Bond lengths [Å] and angles [°] for **271** (CCDC 222289) 434

Appendix 4.8

Table A4.8.1 Atomic coordinates for **274** (CCDC 259858) 444
Table A4.8.2 Selected bond lengths [Å] and angles [°] for **274** (CCDC 259858) 445
Table A4.8.3 Bond lengths [Å] and angles [°] for **274** (CCDC 259858) 445

Appendix 4.9

Table A4.9.1 Atomic coordinates for **288** (CCDC 298214) 453
Table A4.9.2 Selected bond lengths [Å] and angles [°] for **288** (CCDC 298214) 453
Table A4.9.3 Bond lengths [Å] and angles [°] for **288** (CCDC 298214) 453

Appendix 4.10

Table A4.10.1 Atomic coordinates for **289** (CCDC 223628) 459
Table A4.10.2 Selected bond lengths [Å] and angles [°] for **289** (CCDC 223628)..... 459
Table A4.10.3 Bond lengths [Å] and angles [°] for **289** (CCDC 223628) 459

Appendix 4.11

Table A4.11.1 Atomic coordinates for **290** (CCDC 294052) 467
Table A4.11.2 Selected bond lengths [Å] and angles [°] for **290** (CCDC 294052) 467
Table A4.11.3 Bond lengths [Å] and angles [°] for **290** (CCDC 294052) 467

Appendix 5

Table A5.1 Atomic coordinates for **312** (CCDC 243028) 475
Table A5.2 Selected bond lengths [Å] and angles [°] for **312** (CCDC 243028) 476
Table A5.3 Bond lengths [Å] and angles [°] for **312** (CCDC 243028) 476

Appendix 7

Table A7.1 Compounds Appearing in Chapter 2 491
Table A7.2 Compounds Appearing in Chapter 3 493
Table A7.3 Compounds Appearing in Chapter 4 493

LIST OF ABBREVIATIONS

Å	Ångstrom
$[\alpha]_D$	specific rotaton at wavelength of sodium D line
Ac	acetyl
acac	acetylacetonate
AIBN	2,2'-azobisisobutyronitrile
Anal.	analysis
app.	apparent
aq.	aqueous
Ar	aryl
atm	atmosphere
BBN	borabicyclo[3.3.1]nonane
Bn	benzyl
br	broad, broadened
Bu	butyl
i-Bu	isobutyl
n-Bu	*n*-butyl
t-Bu	*tert*-butyl
c	concentration for specific rotation measurements
°C	degrees Celsius
calc'd	calculated
cat.	catalytic

CDI	carbonyldiimidazole
comp	complex
conv	conversion
Cy	cyclohexyl
δ	chemical shift
d	doublet
dba	dibenzylideneacetone
DIBAL	diisobutylaluminum hydride
DHP	dihydropyran
DMAP	4-dimethylaminopyridine
DMF	*N*,*N*-dimethylformamide
DMSO	dimethylsulfoxide
dppe	1,2-bis(diphenylphosphino)ethane
dr	diastereomeric ration
ee	enantiomeric excess
EI	electrospray ionization
elim.	elimination
equiv	equivalents
er	enantiomeric ratio
esd	ellipsoid
Et	ethyl
FAB	fast atom bombardment
g	gram(s)

GC	gas chromatography
[H]	reduction
h	hour(s)
HMDS	hexamethyldisilazane or hexamethyldisilazide
hn	light
HPLC	high performance liquid chromatography
HRMS	high resolution mass spectroscopy
Hz	hertz
IR	infrared
isosp	isosparteine
J	coupling constant
kcal	kilocalories
L	liter or neutral ligand
LAH	lithium aluminum hydride
LDA	lithium dicyclohexylamide
M	metal or molar
m	milli or multiplet or meters
m/*z*	mass to charge ratio
m	micro
Me	methyl
Mes	mesityl
MHz	megahertz
min	minute(s)

mol	moles
mp	melting point
MS	molecular sieves
Ms	methanesulfonyl
N	normal
n	frequency
nbd	norbornadiene
NBS	*N*-bromosuccinimide
NMO	*N*-methylmorpholine *N*-oxide
NMR	nuclear magnetic resonance
NOE	nuclear Overhauser effect
Nuc	nucleophile
[O]	oxidation
o	ortho
OD	outer diameter
OKR	oxidative kinetic resolution
p	para
Ph	phenyl
pH	hydrogen ion concentration in aqueous solution
PhH	benzene
pK_a	acidity constant
ppm	part(s) per million
PPTs	pyridinium *p*-toluenesulfonate

i-Pr	isopropyl
py	pyridine
pyr	pyridine
q	quartet
ref	reference
R_F	retention factor
R_S	small alkyl group
R_L	large aryl or allyl group
s	singlet or selectivity factor
sat.	saturated
sp	(–)-sparteine
stoich.	stoichiometric
Sub	substrate
t	triplet
TBAF	tetrabutylammonium fluoride
TBHP	*tert*-butyl hydroperoxide
TBS	*tert*-butyldimethylsilyl
Tf	trifluoromethanesulfonyl
TFA	trifluoroacetic acid or trifluoroacetate
THF	tetrahydrofuran
THP	tetrahydropyran
TLC	thin-layer chromatography
TMEDA	*N*,*N*,*N*',*N*'-tetramethylethylenediamine

TMPDA	*N*,*N*,*N*',*N*'-tetramethylpropylenediamine
TMS	trimethylsilyl
Ts	*p*-toluenesulfonyl or tosyl
TsOH	*p*-toluenesulfonic acid or tosic acid
UV	ultraviolet
v/v	volume to volume
w/v	weight to volume
X	anionic ligand or halide

CHAPTER 1

Palladium(II)-Catalyzed Oxidase-Type Oxidation Reactions

1.1 INTRODUCTION AND BACKGROUND

Oxidation is one of the most fundamental and important processes in nature. A constant supply of oxygen is essential to most living organisms, and plays an essential role in redox processes catalyzed by metalloenzymes. In oxidative processes, O_2 can be the source of an oxygen atom that is transferred to a substrate (Figure 1.1.1, left). The metalloenzymes that catalyze this process often do so via a metal-oxo species in the metalloenzyme, and are classified as *oxygenases*. Members of this class include the cytochrome P-450 enzymes, which are essential to the initial phase of animal metabolism. A cofactor is required to supply protons and electrons. On the other hand, a substrate can act as the proton and electron donor, with O_2 as the acceptor, with no transfer of an oxygen atom to the substrate (Figure 1.1.1, right). Metalloenzymes of this type are classified as *oxidases*, an example of which is cytochrome oxidase, the final

component of the electron transfer chain that enables the body to use O_2 to generate energy. The atoms of O_2 are converted to water or hydrogen peroxide, as protons and electrons are removed from the substrate in a dehydrogenative process.

Figure 1.1.1 Oxygenase and oxidase enzymes.

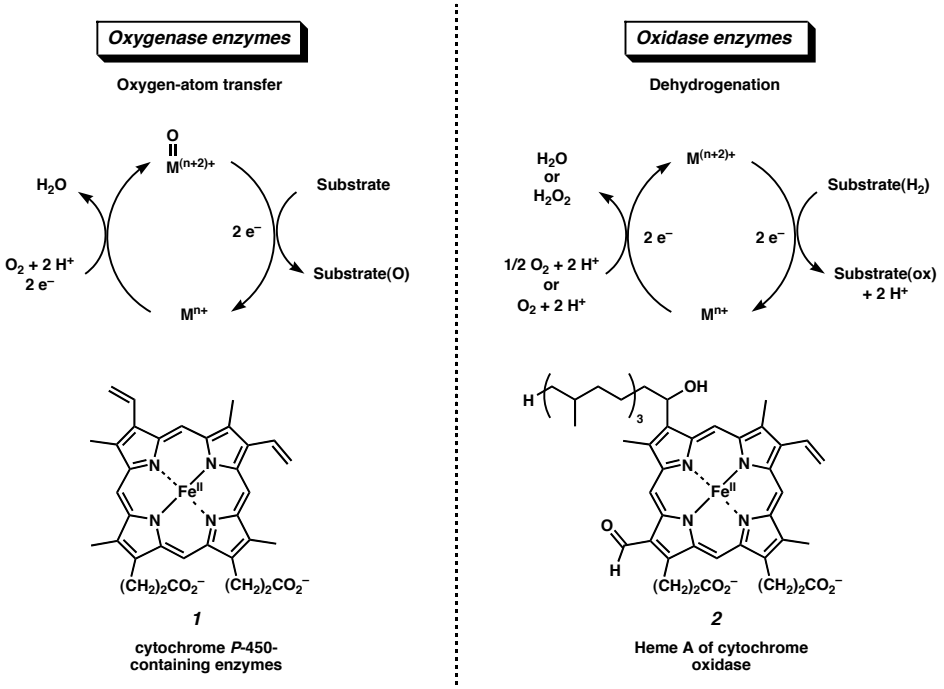

Organic chemists have sought to replicate the high substrate specificity and selectivity exhibited by oxidative metalloenzymes using small molecule catalysis. Through this effort, oxidation has become one of the most effective ways for chemists to induce asymmetry in organic transformations for the production of enantioenriched materials.[1] Most enantioselective oxidations involve the transfer of a heteroatom, commonly oxygen, to a substrate in a manner analogous to that of oxygenase metalloenzymes. Some of the most important examples of reactions of this type are the Sharpless-Katsuki asymmetric epoxidation (**3** → **4**) and the Sharpless asymmetric dihydroxylations (**4** → **5**), or mono- and dioxgenase-type reactions (Figure 1.1.2).[2,3,4]

Figure 1.1.2 Asymmetric oxygenase-type reactions.

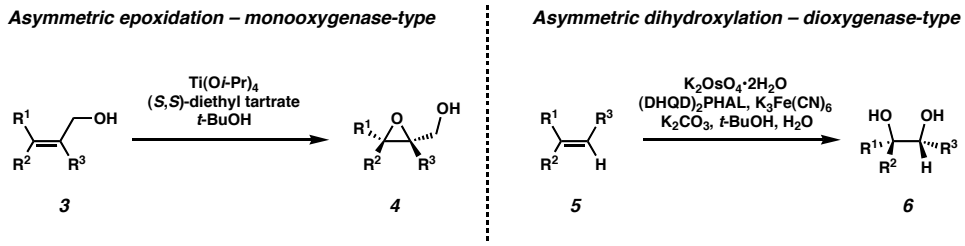

3 *4* *5* *6*

In contrast, there is a significant lack of asymmetric two-electron oxidations that do not involve heteroatom transfer, or which are analogous to the oxidase enzymes. Although racemic reactions of this type, such as alcohol oxidations, alkane dehydrogenations, and aromatic oxidations, are prevalent, there are few asymmetric examples.[5]

1.2 PALLADIUM(II) AS A CATALYST FOR ENANTIOSELECTIVE OXIDASE-TYPE REACTIONS.

Since its inception, the Stoltz laboratory at the California Institute of Technology has been interested in developing asymmetric oxidase-type reactions, in other words, catalytic enantioselective dehydrogenations. Some reactions of this type are shown in Figure 1.2.1. For example, an enantioselective alcohol oxidation would effect a kinetic resolution of a secondary alcohol (**7**) by selective conversion of one enantiomer to ketone (**8**). Oxidative oxygen, nitrogen, or carbon atom cyclizations with appended olefins could occur to produce enantioenriched heterocycles or carbocycles (**9** → **10** or **11** → **12**). Asymmetric aromatic oxidation might also be possible for the synthesis of interesting products or reactive intermediates.

Figure 1.2.1 Potential asymmetric oxidase-type reactions.

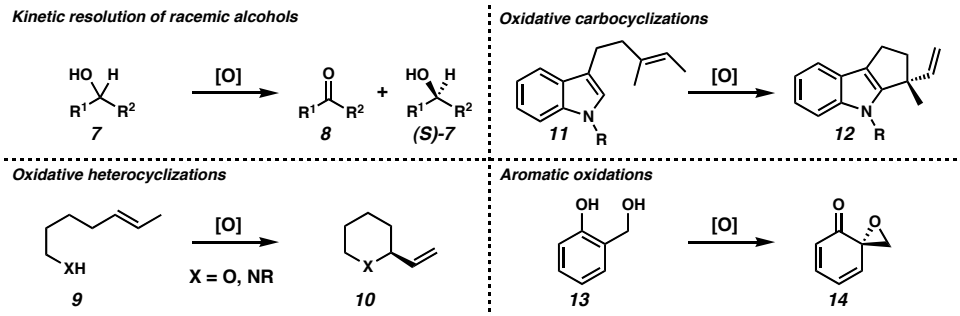

Ideally, a variety of enantioselective dehydrogenations would be carried out by a similar catalyst system, a criterion that would dictate our choice of catalyst. Fortunately, a range of achiral dehydrogenation reactions had been known for several decades for the same transition metal: palladium(II). In the well-known Wacker process, ethylene (**15**) is oxidized to acetaldehyde (**16**) by palladium(II) chloride in the presence of O_2 and a copper cocatalyst (Figure 1.2.2).[6] In 1977, Blackburn and Schwartz reported palladium(II)-catalyzed alcohol oxidation in the presence of sodium acetate and O_2.[7] Because oxidized metal is required for substrate oxidation in these cases, a stoichiometric oxidant is necessary. Both of the above reactions use O_2 as the terminal oxidant in a manner analogous to oxidase enzymes, although the Wacker process requires a copper cocatalyst. Several other reoxidants have been employed, such as peroxides, benzoquinone, and DMSO/O_2, that have enabled the execution of the remainder of the reactions shown in Figure 1.2.2, among others.[8,9] Thus palladium(II) appeared to be an optimal candidate for the development of a suite of asymmetric oxidase-type reactions. This catalyst offered the further advantage of being able to employ O_2 as a stoichiometric oxidant, just as enzymes activate O_2, N_2 and other small molecules as powerful redox reagents.

Figure 1.2.2 Palladium(II)-cataylzed oxidase-type reactions.

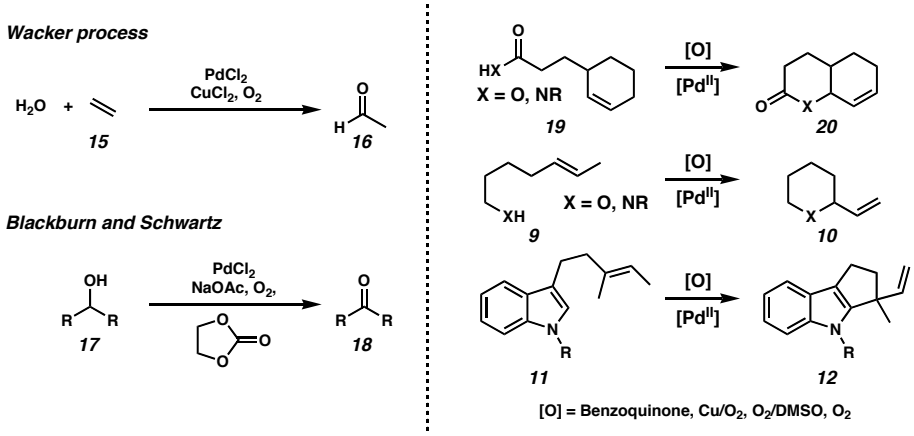

Indeed, over the past six years, our group has realized the potential of palladium(II) to carry out several enantioselective oxidase-type reactions. The kinetic resolution of secondary alcohols, the desymmetrization of meso-diols, and oxidative heterocyclizations have been developed using the same catalytic system: palladium(II) salt, O_2, the chiral ligand (–)-sparteine (**22**), base, and molecular sieves in toluene (Figure 1.2.3). In the course of this work, several interesting questions have arisen regarding the mechanism and selectivity of these processes. Such questions, and the development of oxidative heterocyclizations, are the topic of this thesis.

Figure 1.2.3 Asymmetric palladium(II)-catalyzed oxidase-type reactions.

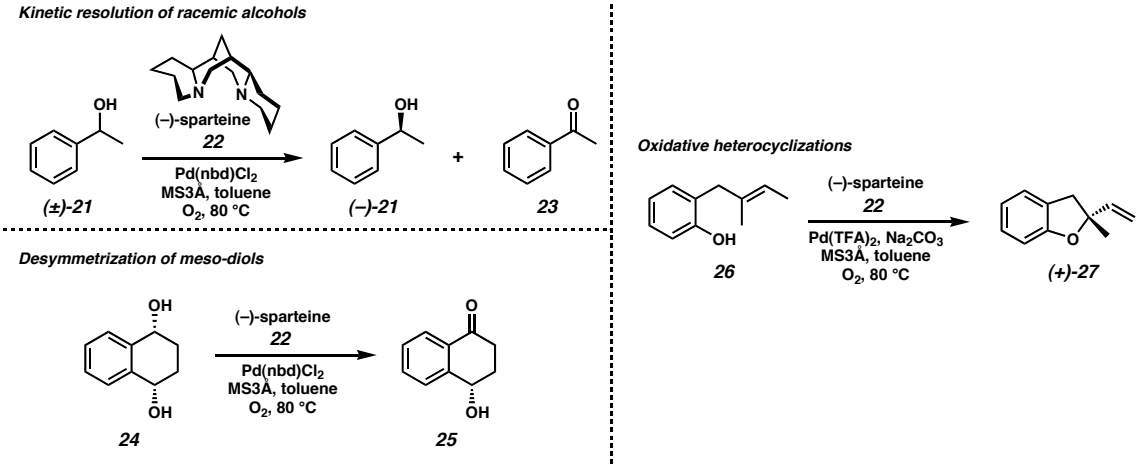

1.3 NOTES AND REFERENCES

[1] (a) Johnson, R. A.; Sharpless, K. B. In *Catalytic Asymmetric Synthesis*; Ojima, I. Ed.; Wiley & Sons, Inc.: New York, 2000, pp 231-280. (b) Katsuki, T. In *Catalytic Asymmetric Synthesis*; Ojima, I., Ed.; Wiley & Sons, Inc.: New York, 2000, pp 287-325. (c) Jacobsen, E. N. In *Comprehensive Asymmetric Catalysis, Vol. 2*; Jacobsen, E. N.; Pfaltz, A.; Yamamoto, H., Eds.; Springer-Verlag: Berlin, 1999, pp 607-618. (d) For a recent review of advances in transition metal catalyzed oxidation, see: Punniyamurthy, T.; Velusamy, S.; Iqbal, J. *Chem. Rev.* **2005**, *105*, 2329-2364.

[2] (a) Katsuki, T. Epoxidation of Allylic Alcohols. In *Comprehensive Asymmetric Catalysis*; Jacobsen, E. N.; Pfaltz, A.; Yamamoto, H., Eds.; Springer-Verlag: Berlin, 1999; Vol. 2, Chapter 18.1, pp 621-648. (b) Johnson, R. A.; Sharpless, K. B. Catalytic Asymmetric Epoxidation of Allylic Alcohols. In *Catalytic Asymmetric Synthesis*; Ojima, I., Ed.; Wiley: New York, 2000; Chapter 6A, pp 231-280.

[3] (a) Markó, I. E.; Svendsen, J. S. Dihydroxylation of Cabon-Carbon Double Bonds. In *Comprehensive Asymmetric Catalysis*; Jacobsen, E. N.; Pfaltz, A.; Yamamoto, H., Eds.; Springer-Verlag: Berlin, 1999; Vol. 2, Chapter 20, pp 713-787. (b) Johnson, R. A.; Sharpless, K. B. Catalytic Asymmetric Dihydroxylation – Discovery and Development. In *Catalytic Asymmetric Synthesis*; Ojima, I., Ed.; Wiley: New York, 2000, Chapter 6D, pp 357-398.

[4] For other examples, including those that involve N-atom transfer, see: (a) Jacobsen, E. N.; Wu, M. H. Epoxidation of Alkenes Other than Allylic Alcohols. In *Comprehensive Asymmetric Catalysis*; Jacobsen, E. N.; Pfaltz, A.; Yamamoto, H., Eds.; Springer-Verlag: Berlin, 1999; Vol. 2, Chapter 6D, pp 649-677. (b) Katsuki, T. Asymmetric Epoxidation of Unfunctionalized Olefins and Related Reactions. In *Catalytic Asymmetric Synthesis*; Ojima, I., Ed.; Wiley: New York, 2000, Chapter 6B, pp 649-677. (c) Jacobsen, E. N. Aziridination. In *Comprehensive Asymmetric Catalysis*; Jacobsen, E. N.; Pfaltz, A.; Yamamoto, H., Eds.; Springer-Verlag: Berlin, 1999; Vol. 2, Chapter 17, pp 607-618.

[5] For general references regarding dehydrogenative oxdations, see: (a) Sheldon, R. A.; Kochi, J. K. *Metal-Catalyzed Oxidations of Organic Compounds*; Academic Press: New York, 1981. (b) Simándi, L. I., Ed. *Dioxygen Activation and Homogeneous Catalytic Oxidation*; Studies in Surface Science and Catalysis; Elsevier: Amsterdam, 1991. (c) Stoltz, B. M. *Chem. Lett.* **2004**, *33*, 362-367. (d) Stahl, S. S. *Angew. Chem. Int. Ed.* **2004**, *43*, 3400-3420. (e) Sigman, M. S.; Schultz, M. J. *Org. Biomol. Chem.* **2004**, *2*, 2551-2554. (f) For a recent review of Pd-catalyzed alcohol oxidation, see:

Muzart, J. *Tetraherdon* **2003**, *59*, 5789-5816. (g) Trost, B. M. *Acc. Chem. Res.* **1990**, *23*, 34-42. (h) Hegedus, L. S. *Tetrahedron* **1984**, *40*, 2415-2434. (i) Hosokawa, T.; Murahashi, S.-I. *Acc. Chem. Res.* **1990**, *23*, 49-54. (j) Semmelhack, M. F.; Kim, C.; Zhang, N.; Bodurow, C.; Sanner, M.; Dobler, W.; Meier, M. *Pure. Appl. Chem.* **1990**, *23*, 2035-2040. (k) Tsuji, J. *Palladium Reagents and Catalysts*; John Wiley & Sons, Ltd.: Chichester, UK, 1995, pp 125-527. (l) Zeni, G.; Larock, R. C. *Chem. Rev.* **2004**, *104*, 2285-2309. (k) Wolfe, J. P.; Thomas, J. S. *Curr. Org. Chem.* **2005**, *9*, 625-655.

[6] Smidt, J.; Hafner, W.; Jira, R.; Sedlmeier, J.; Sieber, R.; Rüttinger, R.; Kojer, H. *Angew. Chem.* **1959**, *71*, 176-182.

[7] (a) Schwartz, J.; Blackburn, T. F. *J. Chem. Soc., Chem. Commun.* **1977**, 157-158. (b) For the earliest example of alcohol oxidation by palladium, see: Wieland, H. *Ber. Dtsch. Chem. Ges.* **1912**, *45*, 484-493.

[8] See Chapter 2, Section 1.1.2, and references therein.

[9] For achiral oxidative carbocyclizations, see: (a) Ferreira, E. M.; Stoltz, B. M. *J. Am. Chem. Soc.* **2003**, *125*, 9578-9779. (b) Zhang, H.; Ferreira, E. M.; Stoltz, B. M. *Angew. Chem. Int. Ed.* **2004**, *43*, 6144-6148.